Morato-Godino, A., Sánchez-Delgado, S., García-Hernando, N. & Soria-Verdugo, A. (2018). Pyrolysis of Cynara cardunculus L. samples – Effect of operating conditions and bed stage on the evolution of the conversion. *Chemical Engineering Journal*, vol. 351, pp. 371–381.

DOI: 10.1016/j.cej.2018.06.114

Pyrolysis of *Cynara cardunculus* L. samples – Effect of operating conditions and bed stage on the evolution of the conversion

Morato-Godino, A.*, Sánchez-Delgado, S., García-Hernando, N., Soria-Verdugo, A.

Carlos III University of Madrid (Spain), Energy Systems Engineering Group, Thermal and Fluids. Engineering Department. Avda. de la Universidad 30, 28911, Leganés (Madrid, Spain).

** corresponding author: amorato@ing.uc3m.es* (Morato-Godino, A.) *Tel: +34 916246032.*

Abstract

The effect of different parameters on the pyrolysis of *Cynara cardunculus* L. was studied through an innovative technique based on a precision scale, capable of measuring the time evolution of the biomass samples mass during their thermochemical conversion process while moving freely inside a fluidized bed. A silica sand bed reactor, operated under different values of excess gas velocity and reactor temperature, was employed to hold the pyrolysis reaction of cardoon particles of three different size ranges. The pyrolysis was accelerated for higher excess gas velocities, obtaining pyrolysis times as short as 17.3 s for experiments conducted under bubbling fluidized bed regimes, compared to 185.9 s required to complete the pyrolysis of the same sample in a fixed bed configuration. Similarly, the effect of increasing the reactor temperature promoted faster heating rates across the fuel samples, especially under fixed bed configurations, for which the pyrolysis time is reduced from 321.7 s to 132.0 s when increasing the bed temperature from 450 to 650 ºC. Regarding the biomass particle size, small sizes are preferred to minimize the conduction thermal resistance inside the fuel particles and, thus, reduce pyrolysis times and increase volatile yields for the pyrolysis in a bubbling fluidized bed reactor. The opposite result was found

when the pyrolysis took place in non-bubbling beds, where the use of larger particles is beneficial to accelerate the biomass pyrolysis reaction.

Keywords: Biomass pyrolysis; Fluidized bed; Devolatilization; Particle size effect; Temperature effect; Heating rate.

Notation

d_{bm}	particle diameter of the bed material [m]
d_i	inner diameter of the reactor [m]
D_{pellet}	diameter of *Cynara cardunculus* L. pellets [m]
g	gravitational acceleration [m/s^2]
h	height of the reactor [m]
h_b	height of the fixed bed [m]
k	apparent rate coefficient [s^{-1}]
L_{pellet}	length of *Cynara cardunculus* L. pellets [m]
m	mass of the sample at time t [kg]
m_0	initial mass of the sample [kg]
m_{vol}	mass of volatiles in the sample [kg]
t	time [s]
t_{pyr}	pyrolysis time [s]
T	reactor temperature [K]
U	gas velocity [m/s]
U_{mf}	minimum fluidization velocity [m/s]
V_{tot}	percentage of total volatile content released [%]
X	percentage of mass of the sample [%]
X_{res}	percentage of solid residue [%]
ε	void fraction of the bed material [–]

ϕ	sphericity of the dense phase particles [–]
α	conversion factor [%]
μ_g	gas dynamic viscosity at reactor temperature [kg/(m·s)]
ρ_{bm}	particle density of the bed material [kg/m^3]
ρ_g	gas density at reactor temperature [kg/m^3]

1. Introduction

Pyrolysis, which consists in the thermal decomposition of solid fuels in a non-oxidative atmosphere at elevated temperatures, is a favorable thermochemical process for biomass conversion, since it enhances the production of a brown-dark liquid called bio-oil, with a lower heating value (LHV) around 14-18 MJ/kg [1]. This bio-oil can be readily stored and transported, permitting its decentralized usage as a fuel in turbines, boilers, and engines or as a source for chemicals production [2,3]. In addition to the bio-oil generated, charcoal and permanent gases are also produced during the pyrolysis of biomass. The physico-chemical properties and the yields of the bio-oil, the permanent gases and the solid residue are strongly affected by the composition of the feedstock, the use of pretreatment techniques for biomass [4, 5], and the operating conditions selected for the pyrolysis process, i.e., reactor temperature, heating rate, biomass particle size, or pyrolysis vapor residence time [6, 7].

Temperature is considered the most sensitive parameter for pyrolysis, influencing significantly the production of the different pyrolysis products [8]. Previous studies have demonstrated that liquid production can be maximized under certain operating conditions, attaining up to 75 wt.% on a dry basis for the pyrolysis of wood in a temperature range of 480-520 °C [6]. Nevertheless, the maximum liquid yield depends not only on the pyrolysis conditions employed, but also on the feedstock. According to the specific literature, the

optimal temperature interval to produce liquid fuel from the pyrolysis of different biomass species ranges from 450 to 650 °C [9,10,11]. Above this temperature range, the released pyrolysis vapors may undergo secondary cracking reactions, decreasing the liquid yield in favor of permanent gas production [12]. Besides, other research studies have assessed the effect of temperature on the other pyrolysis products, i.e., char and permanent gas. Several authors [13,14,15] have found a reduction of the solid residue remaining after pyrolysis, i.e., an improvement of the conversion, for increasing reactor temperatures due to the higher thermal energy available.

The effect of heating rate of biomass particles on the pyrolysis reaction has also been studied by many researchers [7]. It is widely accepted that rapid heating of biomass samples is required to enhance liquid production [16,17,18,19]. Biomass particle size also influences the pyrolysis process due to heat and mass transfer effects inside the solid particle [20]. The use of biomass particle sizes under 2 mm was recommended by Bridgwater et al. [6] to reduce thermal conduction effects inside fuel particles and enhance bio-oil yields when the pyrolysis occurs in fluidized bed reactors. Regarding experimental works, the most common conclusion is that a decrease in biomass particle size leads to larger conversion degrees and liquid yields [21,22,23].

Considering the effects of the above-mentioned parameters on the pyrolysis of lignocellulosic biomass, an accurate control of the operating conditions is required to improve the conversion efficiency and maximize liquid yields. Fluidized beds are widely employed in the thermochemical conversion of biomass since they enable an easy control of the operating conditions of the chemical reactions. This technology provides high heat and mass transfer coefficients due to the contact between fuel particles and bed material [2]. In fact, the convection heat transfer coefficient of a fixed bed increases substantially when the gas velocity is increased above the minimum fluidization velocity [24]. In addition,

the high thermal inertia of the solid particles that conformed fluidized beds permits the isothermal operation, even when holding exothermic or endothermic chemical reactions.

Thermochemical conversion in fluidized bed reactors requires a proper fuel mixing with the bed material to maximize the heat transfer and, thus, increase the efficiency of the process. The effect of the superficial velocity of the fluidizing gas on this mixing has been studied by several authors. Rowe and Nienow [25], who studied particle mixing and segregation in fluidized beds, reported a better solid mixing as the excess gas velocity was increased. This conclusion was also attained by Bilbao et al. [26], who found more homogenous straw/sand mixtures for higher gas velocities. Soria-Verdugo et al. [27,28], applying digital image analysis to study the motion of fuel particles in a pseudo 2D fluidized bed, concluded that the axial mixing increased with the gas velocity, obtaining homogeneous mixing for gas velocities around three times the minimum fluidization velocity even for low density fuel particles, for which the buoyancy force obtained is overcome by the increase of the drag force for higher gas velocities. This result was confirmed for lab-scale 3D fluidized beds by Soria-Verdugo et al. [29] and Lundberg et al. [30].

This work investigates the effects of variations in reactor temperature, biomass particle size, and excess gas velocity on the pyrolysis of *Cynara cardunculus* L. (cardoon) samples in a silica sand bed reactor using an innovative measuring system. The time evolution of the mass of cardoon remaining inside the reactor during the pyrolysis was measured by a precision scale, capable of detecting the mass released by the sample during its conversion while moving freely inside the reactor. The effects of temperature, excess gas velocity, and biomass particle size were studied, analyzing the synergies between the operating parameters and the reactor bed regime. The optimal excess gas velocity for the conversion of cardoon was also determined based on the measured pyrolysis time.

2. Theoretical background

Biomass pyrolysis is a complex process involving a huge number of reactions which are either parallel or consecutive. Therefore, a detailed model of the biomass pyrolysis kinetics would result in a tedious process. In this regard, Reschmeier et al. [31] proposed a simplified model to describe the apparent kinetics of biomass pyrolysis, for which, assuming a first-order reaction, the variation of mass of the sample, m, with time, t, is proportional to the mass of volatiles remaining in the sample, $m_{vol}(t)$, and the apparent rate coefficient, k:

$$\frac{dm}{dt} = -k \cdot m_{vol}(t). \tag{1}$$

Considering that the mass of the sample, m, can be expressed as the sum of the mass of volatiles, $m_{vol}(t)$, and the mass of solid residue, m_{res}, at any time, i.e., $m = m_{vol} + m_{res}$, Eq. (1) can be integrated obtaining the following expression for the time evolution of the mass of the sample:

$$m = m_{vol}(0) \cdot \exp\left(-k \cdot t\right) + m_{res}, \tag{2}$$

where $m_{vol}(0)$ is the total mass of volatiles contained in the sample.

Dividing Eq. (2) by the initial mass of the sample, m_0, and considering that the percentage of solid residue at the end of the pyrolysis process, X_{res}, can be calculated from the total percentage of volatile matter of the sample, V_{tot}, as $X_{res} = 100 - V_{tot}$, the time evolution of the mass percentage of the sample can be determined as:

$$X = 100 + V_{tot} \cdot \left[\exp\left(-k \cdot t\right) - 1\right]. \tag{3}$$

This expression was found to be accurate to describe the pyrolysis of small particles of dry sewage sludge in a bubbling fluidized bed reactor by Soria-Verdugo et al. [32], provided that the effects of heat and mass transfer in the sample are slight.

3. Materials and methods

3.1. Experimental facility

The pyrolysis experiments were conducted in a cylindrical reactor made of stainless steel, with an inner diameter, d_i, of 4.7 cm and a height, h, of 50 cm, operating at atmospheric pressure. The energy required to reach the desired pyrolysis temperature was supplied by three electric resistors, surrounding the reactor, capable of supplying a maximum thermal power of 1.2 kWt.

The absence of oxygen required for the pyrolysis reaction was ensured using Nitrogen as fluidization agent. The Nitrogen flowrate was controlled by a flow regulator and measured by a digital flowmeter PFM710-C6-E from SMC, with a measurement range from 0.2 to 10 l/min. The reactor was placed on a precision scale PS 6000 R2 from RADWAG. The weight measurements conducted during the pyrolysis tests were below the minimum weighting requirement of the scale for all the cases analysed. Furthermore, the accuracy of the weight measurements registered by the scale met the accuracy requirements during the pyrolysis tests. Figure 1 shows a schematic of the facility, further details of the system can be found in [32].

The reactor temperature was measured by a type-K thermocouple immersed in the bed until reaching the desired temperature. Once the desired temperature was attained, the thermocouple was removed to prevent the perturbation of the signal registered by the scale, and the flowrate of Nitrogen was adjusted with a value corresponding to a specific excess

gas velocity. Then the pyrolysis occurred and the vapors released were absorbed by a fume extractor placed above the reactor.

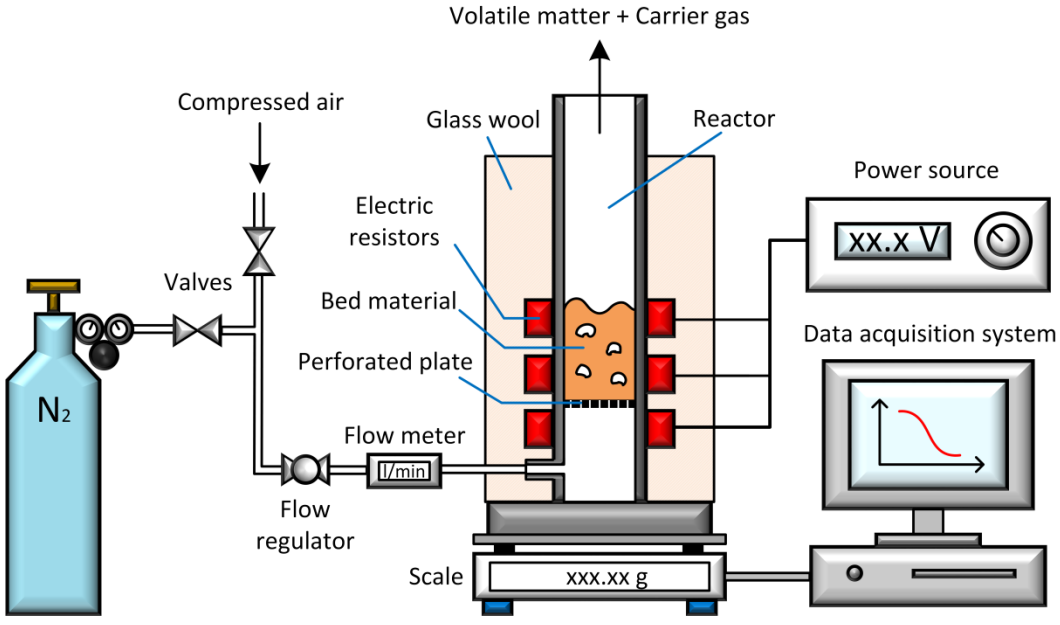

Figure 1. Schematic of the experimental facility.

3.2. Experimental procedure

The experiments consisted in recording the mass signal registered by the precision scale on which the reactor rested while the pyrolysis of cardoon occurred inside the bed. The experimental process was composed of two stages: a first one to reach the desired pyrolysis temperature and a second one in which the biomass conversion occurred while the scale monitored and recorded the weight loss. In the former stage, air was used as fluidization agent for the reactor heating with the thermal power supplied by the three electric resistors until the desired temperature for the run was reached. Once the desired temperature was attained, the fluidization flow was switched to Nitrogen and the flow was adjusted to a value corresponding to a specific excess gas velocity. After removing the thermocouple from the bed and taring the scale, the recording of the weight started and a mass of around 10 g of

cardoon, previously dried at 105 °C in a universal oven UFE 500 from Memmert to remove the moisture content, was introduced at the top of the reactor in a batch.

The influence of three operating parameters, which are gas velocity, bed temperature, and biomass particle size, on the evolution of the mass remaining inside the reactor during the *Cynara cardunculus* L. pyrolysis was analyzed. The experiments were performed at three different temperatures, T (450, 550, and 650 ºC), three biomass particle sizes, and five different flows for N_2, corresponding to five excess gas velocities, $U - U_{mf}$ = -2, 0, 3.5, 7, 10.5 cm/s, and resulting in different regimes: fixed bed, bed at incipent fluidization, and three different regimes of bubbling fluidized bed [33]. The three biomass particle sizes tested are: small size (0.85 – 1.25 mm), medium size ($L_{pellet} \approx D_{pellet}$), and large size ($L_{pellet} \approx 3\ D_{pellet}$), where L_{pellet} and D_{pellet} are the length and the diameter of the cardoon pellets, respectively. The diameter of the cardoon pellets was D_{pellet} = 6 mm. The same values of the excess gas velocity were used for the different tests to obtain similar bubbles' properties, whose motion induced a similar distribution of biomass particles in the bed.

The combination of these variable operating parameters results in 45 different experimental conditions, shown in Table 1. The effects of reactor temperature and biomass particle size on the pyrolysis process were investigated by comparing the cases from different experimental conditions. In contrast, the effect of the excess gas velocity was studied comparing the experiments from the same campaign, i.e., maintaining the same reactor temperature and biomass particle size. The pyrolysis experiments corresponding to each operating condition were replicated to test the repeatability of the experimental procedure followed, attaining deviations lower than 5% in all cases.

Table 1. Operating conditions used during the pyrolysis experiments.

Experimental campaign	Reactor temperature, *T* [°C]	Biomass particle size	Excess gas velocity, $U - U_{mf}$ [cm/s]
1	450	Small	-2, 0, 3.5, 7, 10
2		Medium	
3		Large	
4	550	Small	-2, 0, 3.5, 7, 10
5		Medium	
6		Large	
7	650	Small	-2, 0, 3.5, 7, 10
8		Medium	
9		Large	

3.3. Minimum fluidization velocity

Silica sand was used as bed material in the reactor due to its inert behavior during the pyrolysis of biomass [34]. The minimum fluidization velocity was estimated employing the correlation of Carman-Kozeny [35]:

$$U_{mf} = \frac{\left(\phi d_{bm}\right)^2 \left(\rho_{bm} - \rho_g\right) g}{180 \mu_g} = \frac{\varepsilon^3}{1-\varepsilon} \quad (4)$$

where g is the gravitational acceleration; ε is the void fraction of the dense phase particles; ρ_{bm}, ϕ, and d_{bm} are the density, sphericity, and diameter of the bed material, respectively; and ρ_g and μ_g are the density and dynamic viscosity of the fluidization gas, respectively.

The density of silica sand particles, ρ_{bm}, was 2600 kg/m^3 and the particle diameter, d_{bm}, was in the range of 180-600 μm, belonging to type B solids according to Geldart's classification [36]. A mass of 250 g of silica sand was used in each test, reaching a fixed bed height, h_b, of 10 cm, corresponding to a bed aspect ratio, h_b/d_i, of 2 and a void fraction, ε, of 0.44. The entrainment of bed material particles was prevented by using a reactor height 5 times larger than the fixed bed, removing the fines from the bed material, and limiting the maximum gas

velocity employed in all cases to at least half the terminal velocity of the finest sand particles used, i.e., 180 μm.

Temperature dependence for both density and dynamic viscosity of the gas was considered to estimate the minimum fluidization velocity of the bed material inside the reactor, assuming Nitrogen as an ideal gas, as proposed by Sanchez-Prieto et al. [37].

The minimum fluidization velocity of silica sand particles was also measured in the reactor for temperatures up to 650 °C to evaluate the validity of the correlation of Carman-Kozeny. The measurement was performed by visual inspection of the bed surface to detect the presence of bubbles. The minimum bubbling velocity detected coincides with the minimum fluidization velocity for particles type B according to the Geldart classification, such as the sand particles employed as bed material during the pyrolysis experiments [33]. The measurement was conducting for reducing values of the gas flowrate, from a vigorous bubbling fluidized bed to a fixed bed stage, to prevent the effect of cohesive forces between particles on the minimum fluidization velocity. Figure 2 shows the experimental values of the minimum fluidization velocity together with the estimation of the Carman-Kozeny correlation. The correlation shows a high accuracy to estimate the minimum fluidization velocity of silica sand particles, considering a mean particle diameter, d_{bm}, of 390 μm and a sphericity, ϕ, of 0.64, which is a common value for irregular silica sand particles [33].

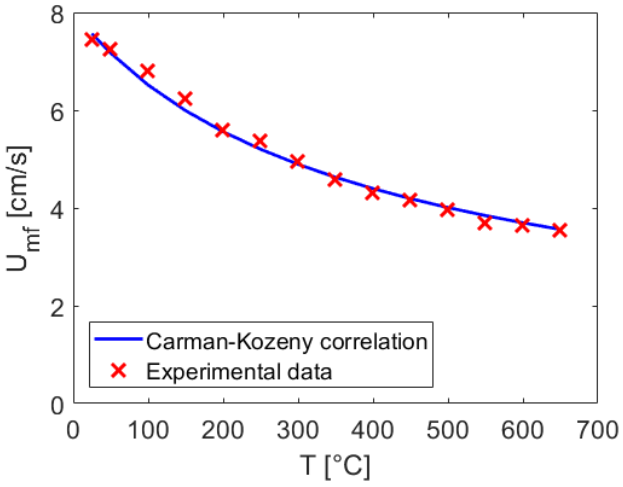

Figure 2. Minimum fluidization velocity of the silica sand particles as a function of reactor temperature.

3.4. *Cynara cardunculus* L. characterization

Cynara cardunculus L. or cardoon is a non-food crop from Mediterraneous regions widely used as a biofuel in thermochemical conversion applications [38,39,40,41,42]. Proximate and ultimate analyses were carried out to characterize the cardoon used in the pyrolysis experiments.

Proximate analysis was conducted in a TGA Q500 from TA Instruments, obtaining the moisture, volatile matter, ash, and fixed carbon contents of the samples. A mass of 10 ± 0.5 mg of cardoon, previously crushed and sieved to a particle size under 100 μm, was employed to avoid heat and mass transfer effects inside the sample during the analysis. A Nitrogen flow of 60 ml/min was supplied to the furnace to guarantee an inert atmosphere. The moisture content was obtained by measuring the final mass loss after an isothermal process at 105 °C, whereas the volatile matter content corresponded to the mass loss after maintaining the sample at 900 °C in an inert atmosphere until no mass variation was observed. The ash content was determined as the remaining mass after the combustion of the sample at 550 °C. The fixed carbon content was finally obtained by difference.

Ultimate analysis was performed using an elemental analyser LECO TruSpec CHNS. Table 2 shows the results of the proximate and ultimate analyses of the *Cynara cardunculus* L. samples, which are similar to those found in literature for this biomass [38,40,41,43]. Further details of the equipment employed to conduct the proximate and ultimate analyses of the samples can be found in [44].

Table 2. Characterization of *Cynara cardunculus* L. samples (ar: as received; db: dry basis; *: obtained by difference).

Proximate analysis [wt.% ar]	
Moisture	5.72
Volatile matter	74.50
Fixed carbon*	12.29
Ash	7.49
Ultimate analysis [wt.% daf]	
C	45.36
H	6.63
N	2.65
S	0.18
O*	45.18

4. Results and discussion

4.1. Effect of excess gas velocity on pyrolysis process

As stated in the introduction, an increase of the excess gas velocity in a bubbling fluidized bed reactor promotes heat transfer by increasing the convection coefficient in the bed [24]. Furthermore, a higher visible bubble flow is also obtained when increasing the excess gas velocity [45] and, thus, larger and more numerous bubbles are found in the bed. These larger bubbles produce a more vigorous fluidization of the bed, which enhances the axial mixing of fuel particles, even for fuel particles with a different density from the dense bed, for which buoyancy forces appear [29,30]. Therefore, the effect of the excess gas velocity on the heat transfer and on the axial mixing of fuel particles, previously studied in the literature, will affect

the reaction rate of biomass during its pyrolysis. To study the effect of the excess gas velocity on the pyrolysis of *Cynara cardunculus* L., the experimental results obtained for the reactor temperature of 550 ºC and the small particle size will be analyzed in this section.

The mass of biomass particles remaining in the reactor during the pyrolysis process, monitored by the scale, was employed to calculate the time evolution of the percentage of fuel mass remaining in the reactor, *X*, as the ratio between the mass at each time over the initial mass of the batch of biomass particles supplied to the reactor. The results for the time evolution of the percentage of mass remaining in the reactor are depicted in Figure 3 (a) for the various excess gas velocities tested. The signals corresponding to the bubbling fluidized bed cases were filtered using a moving average filter to remove the vibration induced by the motion of bubbles. The filtered signal fitted the average trend of the raw signals registered by the precision scale. Further details of this filtration process can be found in a previous work [46].

Figure 3 (a) shows a rapid decrease of the percentage of mass remaining in the reactor for all the excess gas velocities tested, motivated by the release of pyrolysis vapors, composed of condensable and permanent gases, during the thermal decomposition of the solid biomass sample. Two different configurations are shown in Figure 3 (a) depending on the value of the excess gas velocity: for $U - U_{mf} \leq 0$ cm/s, i.e., for a fixed bed or an incipient fluidization regime, and for $U - U_{mf} > 0$ cm/s, corresponding to a bubbling fluidized bed regime. In the former case, when $U - U_{mf} \leq 0$ cm/s, the batch of biomass particles supplied at the top of the reactor rests stationary over the bed surface, forming a package of biomass particles. In contrast, in the latter case, the presence of bubbles in bubbling fluidized beds, when $U - U_{mf} > 0$ cm/s, promotes the dispersion of the biomass particles throughout the whole reactor, enhancing the axial mixing of fuel particles in the bed. This difference in the configuration and location of the biomass particles in the bed affects significantly the time

evolution of the percentage of mass remaining in the reactor during the pyrolysis reaction, presented in Figure 3 (a). For the fixed bed and incipient fluidization regimes ($U - U_{mf} \leq 0$ cm/s), shown as blue curves in Figure 3 (a), the heating rate of the biomass particles is reduced due to conduction heat transfer effects inside the package of particles resting stationary on the bed surface. These conduction heat transfer inside the package of biomass particles delays the pyrolysis reaction compared to the pyrolysis in a bubbling fluidized bed ($U - U_{mf} > 0$ cm/s), shown as black curves in Figure 3 (a), for which the package of biomass particles is dispersed rapidly in the bed by the action of bubbles, and thus, the effect of conduction heat transfer between sample particles is negligible. Furthermore, an increase of the excess gas velocity in the bubbling fluidized bed slightly accelerates the pyrolysis process due to the increase of convection heat transfer coefficients [24] and fuel axial mixing reported in the literature [30].

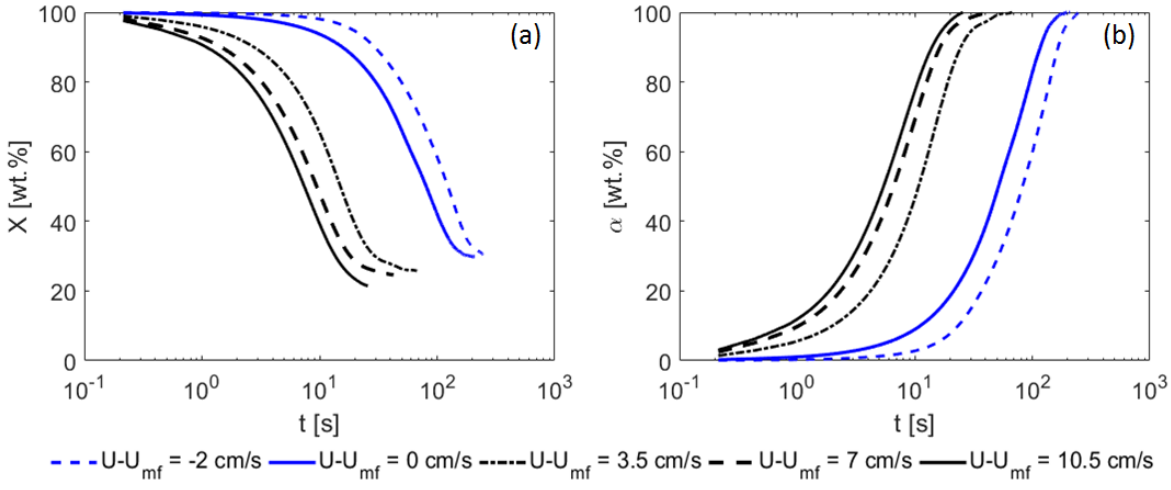

Figure 3. (a) Time evolution of the percentage of mass remaining in the reactor and (b) time evolution of the conversion factor, during the pyrolysis of small particles of *Cynara cardunculus* L. with a bed temperature of 550 °C, for various excess gas velocities.

Figure 3 (a) also shows an effect of the excess gas velocity on the percentage of mass remaining in the reactor, X_{res}, once the pyrolysis of the sample is completed. The total volatile matter released during the pyrolysis can be calculated by difference, as

V_{tot} = 100% – X_{res}. A decrease of the mass remaining, i.e., an increase of the total volatile matter released, can be observed in Figure 3 (a) when increasing the excess gas velocity. The values of the volatile matter released during the complete pyrolysis process, V_{tot}, are reported in Table 3 for each excess gas velocity. A variation of V_{tot} between 69.6% for the fixed bed configuration and 78.6% for the bubbling fluidized bed with the maximum excess gas velocity tested was obtained. The increase of the total volatile matter released with the excess gas velocity may be attributed to the higher heating rates of the fuel particles obtained due to the higher convection coefficients and axial mixing rates. The increase of the volatile matter released for higher particle heating rates is in agreement with the findings of Bridgwater et al. [6] and Yan et al. [47].

The effect of the different percentage of mass remaining in the reactor for each excess gas velocity can be avoided by calculating the conversion factor, α, from the percentage of mass remaining in the reactor, X, to improve the comparison between the curves obtained for each excess gas velocity. Considering the percentage of mass remaining after the pyrolysis process, X_{res}, the conversion factor is defined as $\alpha = (100 - X)/(100 - X_{res})$, being 0 wt.% at the beginning of the pyrolysis process and 100 wt.% once the pyrolysis process is completed. The time evolution of the conversion factor can be found in Figure 3 (b) for the various excess gas velocities tested. In this figure, a displacement of the conversion factor curves to shorter times when increasing the excess gas velocities can be observed, as a result of the higher heating rates of fuel particles. A remarkable effect of the excess gas velocity is observed again between the fixed bed/incipient fluidization and the bubbling fluidized bed regimes, due to the dispersion of fuel particles throughout the whole reactor in the latter case, promoted by the motion of bubbles. A further increase of the excess gas velocity for the bubbling fluidized bed regime accelerates the pyrolysis process slightly

because of the higher convection heat transfer coefficients and axial mixing of biomass particles.

The conversion factor curves for each excess gas velocity permits the calculation of the pyrolysis time, t_{pyr}, as the time required to attain a specific value for the conversion factor. Depending on the application, the value of the conversion factor used to define the pyrolysis time may differ. In this work, a value for the conversion factor equal to 95 wt.% was selected to calculate the pyrolysis time for each operating condition. The values of the pyrolysis time for the pyrolysis of small particles of *Cynara cardunculus* L. at 550 ºC are reported in Table 3, where a substantial reduction in the pyrolysis time of 91% can be observed, from 185.9 s for the fixed bed configuration to 17.3 s for the bubbling fluidized bed regime operated at the maximum excess gas velocity tested.

Table 3. Total volatile matter released and pyrolysis time for the pyrolysis of small particles of *Cynara cardunculus* L. at 550 °C, as a function of the excess gas velocity.

$U-U_{mf}$ [cm/s]	V_{tot} [wt.%]	t_{pyr} [s]
-2	69.6	185.9
0	70.1	134.0
3.5	74.3	31.1
7	75.4	20.4
10.5	78.6	17.3

The optimal biomass feeding rate for each pyrolysis reactor would be inversely proportional to the pyrolysis time obtained. Therefore, a significant increase of the feeding rate can be expected for bubbling fluidized bed reactors compared to fixed beds or incipient fluidized beds. Thus, although an increase of the excess gas velocity from a fixed bed to that of a bubbling fluidized bed involves a higher Nitrogen consumption and a higher pressure drop for the gas circulating through the bed, this higher operating cost is justified by the significant increase of the biomass feeding rate feasible in a bubbling fluidized bed, which results in a substantial increase of the biomass conversion by pyrolysis. However, once the bed is

operated in a bubbling fluidized bed stage, a further increase of the excess gas velocity produces only a slight decrease of the pyrolysis time, i.e., a slight increase of the biomass feeding rate. Hence, the optimal excess gas velocity for the pyrolysis conversion of biomass particles in a bed reactor corresponds to the lowest excess gas velocity for which the bed is operated under a bubbling fluidized bed regime.

The acceleration of the pyrolysis reaction when increasing the excess gas velocity in a bubbling fluidized bed was also found for the rest of reactor temperatures and biomass particle sizes. Therefore, an increase of the excess gas velocity accelerates the pyrolysis process of biomass in a bubbling fluidized bed in the range of excess gas velocity tested in this study.

4.2. Effect of reactor temperature on pyrolysis process

Pyrolysis is an endothermic reaction that converts a solid fuel into volatile gases, remaining a carbonaceous solid residue known as char. Several works have investigated the effect of temperature on the pyrolysis process. Generally, a reduction of the solid residue remaining after the pyrolysis reaction is obtained when increasing the temperature and, thus, the conversion yield is improved for higher temperatures [13,14,15]. This section focuses on the effect of the reactor temperature on the pyrolysis of *Cynara cardunculus* L. samples conformed by particles of small size. Pyrolysis tests were conducted for reactor temperatures, T, of 450, 550, and 650 °C, for various excess gas velocities. Since the pyrolysis experiments were conducted under isothermal conditions and for a constant value of the excess gas velocity, no overestimation of the mass measured by the scale, promoted by variations of the gas pressure drop was detected, in contrast to the non-isothermal pyrolysis measurements performed by Sami and Chaouki [48].

The time evolution of the percentage of mass remaining in the reactor, *X*, for various excess gas velocities is presented in Figure 4 for the three different reactor temperatures, *T*, tested, i.e., 450, 550, and 650 ºC. The end of all the pyrolysis tests is established when the variation of the percentage of mass with time is lower than 0.02% in 1 s. A similar effect of the increase in excess gas velocity is observed for all the reactor temperatures, accelerating the pyrolysis process in all cases. An effect of temperature on the percentage of solid residue obtained when the pyrolysis is completed can be observed in Figure 4. A reduction of the solid residue, i.e., an increase of the total volatile matter released, was obtained when the pyrolysis of *Cynara cardunculus* L. was carried out in a reactor operated at a higher temperature, due to the higher thermal energy available in the reactor, as previously stated by several authors [14,15,49,50,51].

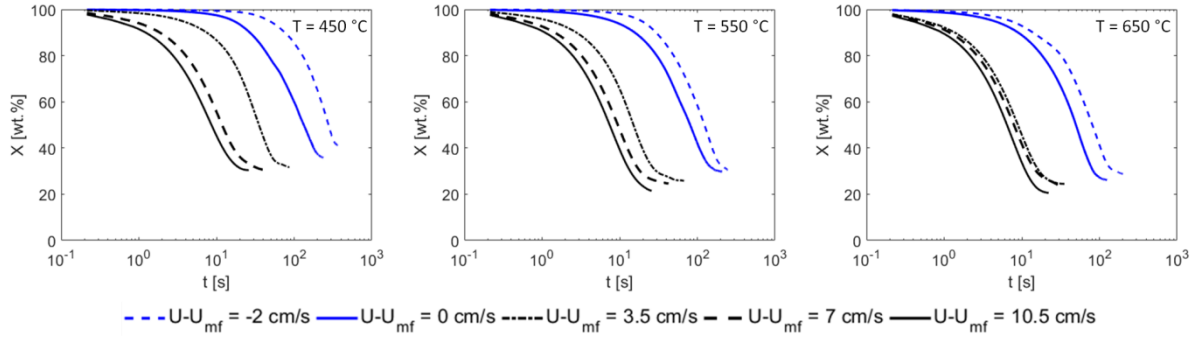

Figure 4. Time evolution of the percentage of mass remaining in the reactor during the pyrolysis of small particles of *Cynara cardunculus* L. for various excess gas velocities and bed temperatures.

From the time evolution of the percentage of mass remaining in the reactor, *X*, shown in Figure 4, the reaction rate, d*X*/d*t*, was calculated as its derivative with time to improve the comparison of the results obtained for the different reactor temperatures. The time evolution of the reaction rate, d*X*/d*t*, is depicted for all excess gas velocities and reactor temperatures in Figure 5. For all the reactor temperatures tested, an increase of the excess gas velocity results in a higher reaction rate, and thus, accelerates the pyrolysis process. As stated above, there is also a substantial difference in the reaction rate for the different

configurations analyzed, obtaining low reaction rates for the fixed bed and incipient fluidization regimes, for which the biomass particles are accumulated on the bed surface, and remarkably higher values of the reaction rate for the bubbling fluidized bed regime, for which the motion of bubbles promotes the dispersion of biomass particles throughout the whole bed height. For the bubbling fluidized bed regime, the effect of temperature is more pronounced for the lowest excess gas velocity corresponding to a bubbling fluidized bed regime, $U - U_{mf}$ = 3.5 cm/s, for which the low-density biomass particles supplied at the top of the bed are more prone to be found at the upper part of the bed due to buoyancy effects [29]. In this case, the higher thermal energy available in this zone of a reactor operated at a higher temperature promotes a faster pyrolysis reaction of the biomass samples because of a higher heating rate of the fuel particles. This effect of the reactor temperature is lower when increasing the excess gas velocity, due to the more vigorous fluidization produced in the bed that counteracts the buoyancy effect, enhancing the mixing of biomass particles throughout the whole bed height.

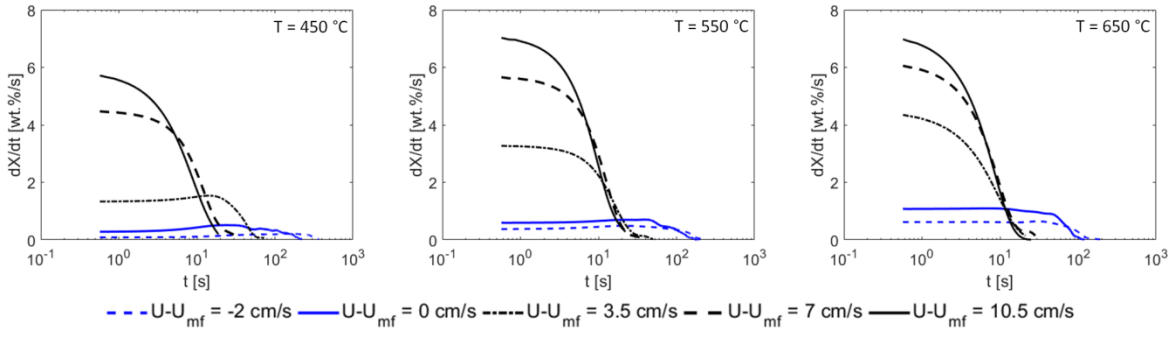

Figure 5. Time evolution of the reaction rate during the pyrolysis of small particles of *Cynara cardunculus* L. for various excess gas velocities and bed temperatures.

Figure 6 (a) shows the total volatile matter released during the pyrolysis of small particles of *Cynara cardunculus* L. in a bed operated at 450, 550, and 650 °C, as a function of the excess gas velocity. The total volatile matter released during the pyrolysis process increases with both the excess gas velocity and the reactor temperature. For an excess gas velocity of *U*

– U_{mf} = - 2 cm/s, corresponding to a fixed bed configuration, an increase of 11.8 wt.% in the conversion yield was attained by increasing the reactor temperature from 450 to 650 ºC; whereas, for an excess gas velocity of $U - U_{mf}$ = 10.5 cm/s, corresponding to a bubbling fluidized bed regime, an increase of 10.1 wt.% in the conversion yield was obtained for the same increase of the reactor temperature. Furthermore, as can be observed in Figure 6 (a), the effect of increasing the reactor temperature on the conversion yield, i.e., on the total volatile matter released, is not linear, being stronger for lower reactor temperatures.

The effect of the reactor temperature on the velocity of the pyrolysis process can be observed by calculating the pyrolysis time, as the time required for the conversion factor, α, to attain a value of 95 wt.%. The results for the pyrolysis time of small particles of *Cynara cardunculus* L. are plotted in Figure 6 (b) as a function of the excess gas velocity, for the various reactor temperatures tested. A remarkable effect of the reactor temperature on the pyrolysis time can be observed for the fixed bed and incipient fluidization regimes, i.e., $U - U_{mf} \leq 0$ cm/s, for which the heat transfer from the pyrolysis medium to the biomass particles is limited due to a reduced contact area between the bed material and the fuel, which formed a package of particles resting stationary on the bed surface. Therefore, the higher thermal energy associated to higher temperatures results in an acceleration of the pyrolysis, due to the higher heating rate of the biomass particles promoted by an increase of the temperature difference between the reactor and the biomass particles. The effect of the reactor temperature is still visible for the lowest excess gas velocity corresponding to a bubbling fluidized bed regime, $U - U_{mf}$ = 3.5 cm/s, for which buoyancy effects on the biomass particles supplied to the bed are still noticeable due to the smooth fluidization produced in the bed. These buoyancy effects forced the biomass particles to move in a restricted part of the bed, close to the bed surface, and thus, the higher thermal energy available in this restricted zone when the bed temperature is higher increases the heating rate of the

particles, reducing the pyrolysis time. This effect of the reactor temperature on the pyrolysis time is reduced for higher excess gas velocities, for which the large bubbles present in the bed increase the drag force on the biomass particles, reducing significantly the effect of buoyancy forces. Hence, the axial mixing of biomass particles is promoted by the increase in excess gas velocities, and once the biomass particles are distributed throughout the bed height, the thermal energy of the whole bed is used to heat up the biomass particles and the effect of bed temperature is lower. In terms of relative variation, a time reduction of 59.0% (189.7 s) was reached by increasing the reactor temperature from 450 to 650 ºC under fixed bed conditions, $U - U_{mf}$ = - 2 cm/s, whereas a time reduction of only 18.2% (3.15 s) was attained for the same temperature increase in a bubbling fluidized bed operated with an excess gas velocity of $U - U_{mf}$ = 10.5 cm/s.

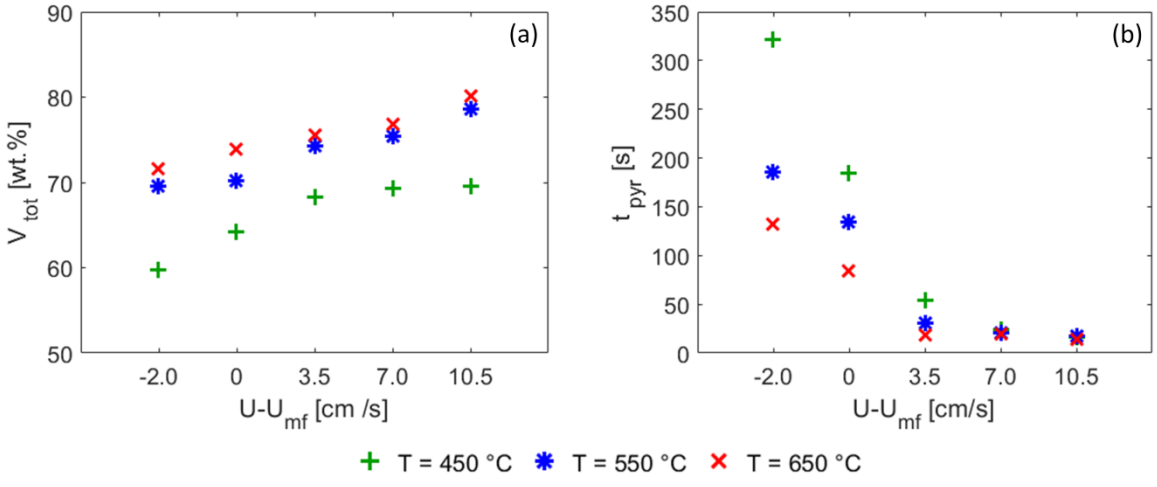

Figure 6. (a) Total volatile matter released and (b) pyrolysis time for the pyrolysis of small particles of *Cynara cardunculus* L. as a function of the excess gas velocity for various reactor temperatures.

The total conversion yields obtained for the small particle size of *Cynara cardunculus* L. in a fixed bed are comparable to those reported by Encinar et al. [38], while the conversion measured in this work for the small cardoon particles in a bubbling fluidized bed are similar to those determined by Coulson and Bridgwater [52].

The enhancement of the pyrolysis process attributed to the temperature increase was found to be independent of the particle size of the biomass samples, since the same results reported for samples conformed by small particles, i.e., larger conversion yields for all excess gas velocities and acceleration of the process at low gas velocities, were observed for the rest of particles sizes.

4.3. Effect of biomass particle size on pyrolysis process

Previous research on the pyrolysis of lignocellulosic biomass has shown that fuel particle size affects significantly the distribution of the three major products obtained from this conversion process, i.e., solid residue (char), liquid, and permanent gases. The common conclusion among these works is a decrease of the solid residue for the use of fine particles, and thus an increase of the conversion yield due to a reduction of heat and mass transfer effects inside the solid particles [22,23,53,54]. In this study, the effect of particle size is evaluated comparing results obtained for the pyrolysis of three different particle sizes: small size (0.85 – 1.25 mm), medium size ($L_{pellet} \simeq D_{pellet}$), and large size ($L_{pellet} \simeq 3\ D_{pellet}$).

The time evolution of the reaction rate, dX/dt, is presented for a reactor temperature of 550 °C and for all the excess gas velocities and biomass particle sizes analyzed in Figure 7. As in the previous sections, the different configurations of the bed affect significantly the evolution of the reaction rate. Higher reaction rates are attained for bubbling bed configurations ($U - U_{mf} > 0$ cm/s) due to a better axial mixing of the biomass, whereas the static behavior of the samples over the bed material during the pyrolysis for the cases of fixed bed and incipient fluidization regimes ($U - U_{mf} \leq 0$ cm/s) resulted in a decrease of the reaction rates. Concerning the pyrolysis at elevated gas velocities ($U - U_{mf} \geq 7$ cm/s), in which the fuel particles are dispersed throughout the whole bed height,

a reduction in the biomass particle size resulted in a significant increase in the reaction rate because of the enhancement of the heating rate of these small particles. In contrast, the effect of reducing particle size on the reaction rate was less pronounced when working under the bubbling fluidized bed regimen with a lower excess gas velocity, i.e., $U - U_{mf} = 3.5$ cm/s. In that case, as previously mentioned, the particles move freely in a restricted zone close to the bed surface due to buoyancy effects and, thus, the heating rate of the particles is limited by the thermal energy available instantaneously in that zone. Therefore, although reducing particle size has a beneficial effect on the conversion process for a bubbling fluidized bed since the heating rate of the particles is enhanced, the limited external heat transfer for low excess gas velocities leads to slight variations on the reaction rate.

The opposite effect was found for non-bubbling bed operations, where reducing particle size resulted in a decrease of the reaction rate. Under these configurations of the bed, $U - U_{mf} \leq 0$ cm/s, for which the biomass rests stationary over the inert bed material forming a package of biomass particles, the samples compactness depends on their particle size. The compactness of smaller particles tends to be higher than for the large pellets, whose shape enhances the appearance of gaps between the pellets conforming the package of particles, through which the hot inert gas employed can easily percolate. Therefore, the effects of interparticle heat transfer inside the package of small particles is significantly higher, delaying the conversion process and enhancing charring reactions. For the pyrolysis of medium and large size particles, the higher percolation of hot inert gas between particles increases their heating rates, resulting in a higher reaction rate. The time evolution of the reaction rate of medium size particles, i.e., small pellets, in a fixed and an incipient fluidization bed shows an increase to reach a maximum reaction rate close to the end of the pyrolysis process. The appearance of this maximum for the reaction rate may be attributed

to a limitation of the particles heating by the thermal conduction inside them, which is enhanced by the lower thermal gradient between the particles' surface and center at low gas velocities due to the lower convection coefficients. The maximum of the reaction rate is observed during the pyrolysis of large pellets for excess gas velocities up to $U - U_{mf} = 3.5$ cm/s, due to the higher importance of thermal conduction inside these coarse particles.

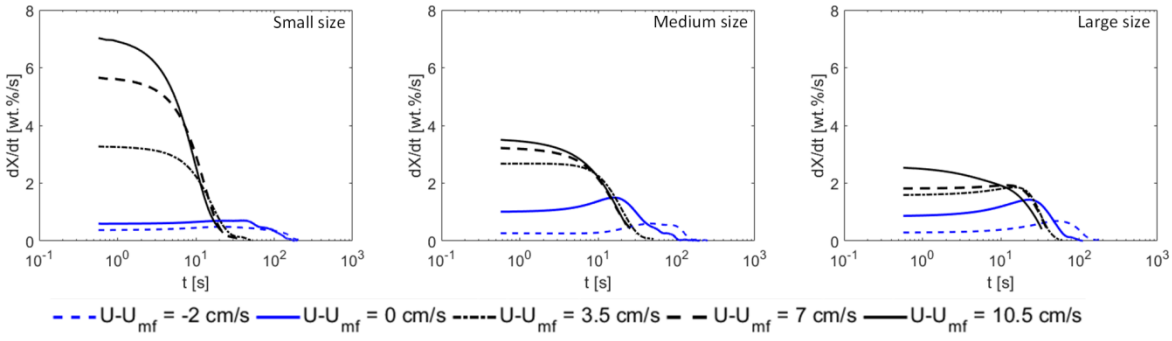

Figure 7. Time evolution of the reaction rate during the pyrolysis of *Cynara cardunculus* L. at 550 ºC for various excess gas velocities and particle sizes.

The total volatile matter released during the pyrolysis of *Cynara cardunculus* L. is depicted in Figure 8 as a function of the excess gas velocity for each temperature and particle size analyzed. The volatile matter released increases with the excess gas velocity independently of the reactor temperature and biomass particle size. In addition, an increase of the volatile matter released, i.e., larger conversion yields, is also obtained for higher reactor temperatures as a result of the higher thermal energy available in the reactor, especially for the increase from 450 to 550 °C, due to the limited thermal energy available at 450 ºC. Regarding the effect of particle size, an enhancement of the conversion yield is found for the use of coarse particles in fixed and incipient fluidization beds due to their higher heating rate promoted by the lower compactness of the package of large particles located on the bed surface. In contrast, the higher compactness of the package of small particles produced for fixed bed and incipient fluidization stages reduces the heating rate of the particles because of the importance of interparticle thermal conduction inside the package, resulting

in lower values of the volatile matter released. This effect is evident for temperatures of 450 and 550 °C, whereas at 650 °C similar values were obtained for the total volatile matter released by small and large particles. In this last case, the heat transfer limitations related to interparticle thermal conduction may be overcome by the larger temperature difference associated to the elevated reactor temperature. The pyrolysis of large particles under fixed bed conditions ($U - U_{mf} = -2$ cm/s) resulted in an increase of the volatile matter released of 3.7wt.%, 0.6 wt.%, and 0.2 wt.% compared to the pyrolysis of small particles, for reactor temperatures of 450, 550, and 650 °C, respectively.

The use of small particles is beneficial when the pyrolysis of *Cynara cardunculus* L. occurs in a bubbling fluidized bed, $U - U_{mf} > 0$ cm/s. At this fluidization stage, for low excess gas velocities, the biomass particles are mixed with the bed material only in the upper part of the bed due to buoyancy effects, however, the external convection on the particles is improved because of a better axial mixing compared to the fixed bed and incipient fluidization configurations. Therefore, in these cases, an increase of the volatile matter production is attained for lower particle sizes, since smaller particles are heated faster and more uniformly, preventing charring reactions. As the excess gas velocity is increased, the fluidization becomes more vigorous and thus the fuel is more dispersed throughout the whole bed height, attaining larger volatile yields for the pyrolysis of samples consisting of small particles; whereas no significant increase in the solid conversion for samples conformed by larger particles is observed. This is caused by the importance of thermal conduction inside the biomass particles, which, in combination with a significant particle size, limits the biomass conversion, resulting in higher residue yields. Therefore, the use of finer particles is recommended to achieve larger conversion yields during the pyrolysis of biomass in a bubbling fluidized bed. For the pyrolysis of *Cynara cardunculus* L., the conversion increases associated to the use of the smallest particle size compared to the largest pellets during the

pyrolysis in a bubbling fluidized bed operated at the maximum excess gas velocity tested, i.e., $U - U_{mf} = 10.5$ cm/s, were 2.5 wt.%, 5.1 wt.%, and 3.5 wt.% for reactor temperatures of 450, 550, and 650 °C, respectively.

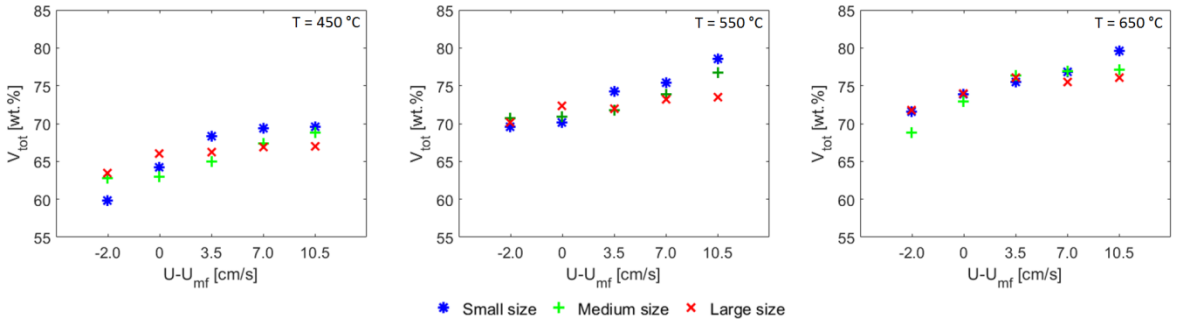

Figure 8. Total volatile matter released during the pyrolysis of *Cynara cardunculus* L. as a function of the excess gas velocity for various reactor temperatures and particles sizes.

The pyrolysis time for the *Cynara cardunculus* L. samples is plotted in Figure 9 as a function of the excess gas velocity for the different reactor temperatures and particle sizes tested. The effect of the excess gas velocity on the pyrolysis time is similar for all the reactor temperatures and particles sizes studied, obtaining a reduction of the pyrolysis time for higher excess gas velocities as a result of the higher heating rates of the biomass particles motivated by the higher axial mixing and convection coefficients. This time decrease with the excess gas velocity is very significant until reaching the bubbling fluidized bed stage, for which the conduction heat transfer limitations between particles are overcome when the package of biomass particles on the bed surface is broken due to the motion of bubbles inside the bed. Further increases of the excess gas velocity once the bubbling fluidized bed regime is attained result only in slight pyrolysis time reductions. The fluidization stage also influences on the effect of the other two parameters, i.e., reactor temperature and particle size, on the time required to complete the pyrolysis process.

Increasing the reactor temperature results in an acceleration of the biomass pyrolysis when the fuel is static forming a package of particles on the bed surface, i.e., for the fixed bed and

incipient fluidization regimes, because of the increase of the heating rate of the particles motivated by the larger temperature difference between the reactor and the biomass. In addition, larger particles are preferred for the pyrolysis experiments conducted under fixed bed and incipient fluidization configurations, since shorter pyrolysis times are obtained due to the higher heating rate attributed to the lower compactness of the package conformed by these coarse particles. Time reductions of 39.6% (127.3 s), 20.2% (37.6 s) and 16.4% (21.7 s) were attained for the pyrolysis of the largest pellets in a fixed bed reactor compared to the pyrolysis of the smallest particles for reactor temperatures of 450, 550, and 650 °C, respectively. In contrast, once the bed is fluidized ($U - U_{mf} > 0$ cm/s) and thus the fuel is mixed with the inert material of the bubbling fluidized bed, increasing the reactor temperature leads to no time reductions. In these scenarios, the limiting factor for the biomass heating is the thermal conduction inside the biomass particles, since the convection at the particle's external surface is enhanced by the fuel mixing with the bed material due to the motion of bubbles and by the higher convection coefficient obtained for higher excess gas velocities. Therefore, the most effective measure to accelerate the pyrolysis of biomass under bubbling fluidized bed regimes is the reduction of particle size, which decreases the effect of thermal conduction, leading to higher heating rates of the biomass particles. The pyrolysis time reductions obtained employing the small particle size instead of the largest pellets were 65.2% (46.4 s), 52.0% (36 s) and 59.3% (34.7 s) for an excess gas velocity of $U - U_{mf} = 0.5$ cm/s and reactor temperatures of 450, 550, and 650 °C, respectively.

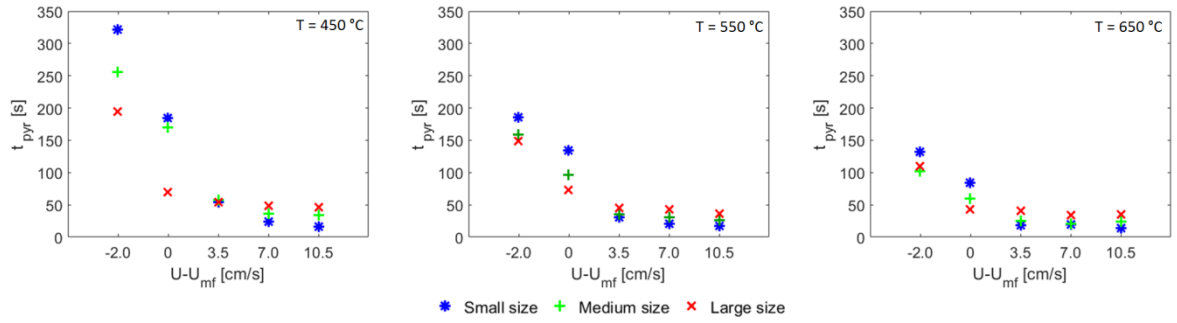

Figure 9. Pyrolysis times of *Cynara cardunculus* L. as a function of the excess gas velocity for samples of different particle sizes and bed temperatures of 450, 550, and 650 °C.

The effect of the particle size on the conversion during the pyrolysis of biomass strongly depends on the fluidization stage under which the pyrolysis is conducted. When the pyrolysis occurs in a fixed or an incipient fluidization bed, where the biomass forms a package of particles resting stationary on the bed surface, the use of large particles accelerates the pyrolysis and results in larger volatile yields because of an enhancement of the biomass particles' heating rate. In contrast, the bubbles' motion characteristic of fluidized beds promotes the axial mixing of the biomass particles with the bed material, enhancing the heating rate of the fuel. When the biomass pyrolysis occurs in a bubbling fluidized bed, the thermal conduction inside the biomass particles is the limiting factor for the thermal degradation process and, thus, a reduction of the biomass particle size results in larger conversion yields and shorter pyrolysis times. Therefore, the use of large biomass particles is advisable when the pyrolysis occurs in a reactor in which the particles form a stationary package; however, when the biomass particles are dispersed and separated from each other, such as in a bubbling fluidized bed, the use of fine particles is recommended to improve the pyrolysis process.

4.4. Apparent kinetics of the pyrolysis process

The apparent kinetics model proposed by Reschmeier et al. [31] was applied to all the pyrolysis measurements conducted in this work for *Cynara cardunculus* L. The comparison

of the experimental results and the estimations of the apparent kinetics model permits the evaluation of the relevance of heat and mass transfer effects during the pyrolysis process. As stated by Soria-Verdugo et al. [32], the apparent kinetics model proposed by Reschmeier et al. [31] is accurate to describe the pyrolysis of biomass, provided that the effects of heat and mass transfer inside the sample are negligible. Therefore, the deviations of the model predictions from the experimental measurements could be attributed to heat and mass transfer effects inside the biomass particles.

The time evolution of the mass percentage measured by the scale, i.e., the experimental X vs t curves, where fitted to the expression obtained from the apparent kinetics model, Eq. (3). For the fitting, the experimental value of the total volatile matter released by the sample, shown in Figure 8, was used. Thus, the only free fitting parameter was the apparent rate coefficient, k, which was obtained for the pyrolysis of *Cynara cardunculus* L. under each operating condition. The results obtained for the apparent rate coefficient, k, for each case are reported in Table 4 together with the determination coefficient of the fitting, R^2, which informs of the accuracy of the apparent kinetics model to describe *Cynara cardunculus* L. pyrolysis.

Table 4. Results of the fitting of the experimental results to the apparent kinetics model.

		450 ºC		550 ºC		650 ºC	
	$U - U_{mf}$ [cm/s]	k [s^{-1}]	R^2 [-]	k [s^{-1}]	R^2 [-]	k [s^{-1}]	R^2 [-]
Small	-2	0.005	0.884	0.010	0.933	0.015	0.958
	0	0.011	0.952	0.016	0.965	0.024	0.956
	3.5	0.037	0.961	0.076	0.981	0.129	0.985
	7	0.107	0.987	0.120	0.989	0.138	0.992
	10.5	0.148	0.988	0.154	0.988	0.164	0.988
Medium	-2	0.007	0.902	0.012	0.917	0.018	0.949
	0	0.012	0.939	0.027	0.962	0.045	0.961
	3.5	0.033	0.915	0.064	0.971	0.089	0.976
	7	0.055	0.950	0.076	0.977	0.098	0.984
	10.5	0.061	0.972	0.083	0.973	0.117	0.982
Large	-2	0.008	0.850	0.013	0.892	0.024	0.971
	0	0.025	0.885	0.028	0.935	0.046	0.943
	3.5	0.030	0.934	0.042	0.935	0.051	0.954
	7	0.033	0.902	0.045	0.934	0.056	0.963

	10.5	0.038	0.916	0.060	0.971	0.070	0.989

The low values of the determination coefficient, R^2, for the fixed and incipient fluidization regimes, independently of the biomass particle size, confirm the importance of heat and mass transfer effects inside the package of particles generated over the bed surface in these cases. Furthermore, although the biomass particles are rapidly dispersed throughout the bed in a bubbling fluidized regime, the R^2 values are also low for the pyrolysis of medium and large particles of *Cynara cardunculus* L. in a bubbling fluidized bed, i.e., $U - U_{mf}$ = 3.5, 7 and 10 cm/s, informing of the relevance of heat and mass transfer effect inside the individual biomass particles. Therefore, the apparent kinetics model proposed is only valid to describe the pyrolysis of small cardoon particles in a bubbling fluidized bed, for which the values of the determination coefficient of the fitting are high (higher than 0.98 in all cases, except for the lower excess gas velocity and lower temperature due to the low energy available in the reactor) as a result of the slight effects of heat and mass transfer inside the small size particles.

5. Conclusions

The pyrolysis process was significantly influenced by the excess gas velocity, especially when different configurations of the bed were obtained. For the fixed and incipient fluidization beds, the biomass particles form a package that rests stationary on the bed surface, whereas in a bubbling fluidized bed the fuel particles are dispersed and mixed with the bed material due to the motion of bubbles, enhancing the heating rate of the fuel and thus its conversion. An increase in the reactor temperature also affects the pyrolysis, resulting in a faster process with a larger conversion yield, as an effect of the increase in the biomass heating rate because of the higher difference in temperature between the fuel and

the reactor, which results in a higher thermal power transferred from the reactor to the fuel particles.

Concerning the biomass particle size, the results were influenced by the fluidization regimen under which the conversion process occurred. Larger particles sizes are preferred for reactors where the biomass particles form stationary packages of particles, since the lower compactness of packages conformed by coarse particles permits a better contact between the particles surface and the hot percolating gas. However, for reactors in which the particles are rapidly dispersed, such as in bubbling fluidized bed reactors, small particle size is recommended to avoid the limiting effect of the thermal conduction inside the particles on their heating rate. The effects of heat and mass transfer on the pyrolysis reactions were quantified by comparing the estimations of a first-order apparent kinetics model to the experimental results. The model was found to be valid to describe the pyrolysis of small particles of *Cynara cardunculus* L. in a bubbling fluidized bed, where heat and mass transfer effects are negligible. However, for larger particles and/or lower excess gas velocities corresponding to a fixed or an incipient fluidization bed, discrepancies were found between the model predictions and the experimental measurements due to heat and mass transfer inside or between the biomass particles.

Acknowledgments

The authors gratefully acknowledge the financial support provided by Fundación Iberdrola (Spain) under the program ‘‘Programa de Ayudas a la Investigación en Energía y Medioambiente”.

References

[1] D. Chen, J. Zhou, Q. Zhang, X. Zhu, Evaluation methods and research progresses in bio-oil storage stability, Renewable and Sustainable Energy Reviews 40 (2014) 69-79.

[2] J. Piskorz, D.S. Scott, I.B. Westerberg, Flash pyrolysis of sewage sludge, Industrial & Engineering Chemistry Process Design and Development (1986) 25, 265-270.

[3] S. Czernik, A.V. Bridgwater, Overview of Applications of Biomass Fast Pyrolysis Oil, Energy & Fuels 18 (2004) 590-598.

[4] D. Chen, J. Mei, H. Li, Y. Li, M. Lu, T. Ma, Z. Ma, Combined pretreatment with torrefaction and washing using torrefaction liquid products to yield upgraded biomass and pyrolysis products, Bioresource Technology 228 (2017) 62-68.

[5] D. Chen, Z. Zheng, K. Fu, Z. Zeng, J. Wang, M. Lu, Torrefaction of biomass stalk and its effect on the yield and quality of pyrolysis products, Fuel 159 (2015) 27-32.

[6] A.V. Bridgwater, D. Meier, D. Radlein, An overview of fast pyrolysis of biomass, Organic Geochemistry 30 (1999) 1479-1493.

[7] D. Chen, J. Zhou, Q. Zhang. Effects of heating rate on slows pyrolysis behavior, kinetic parameters and products properties of moso bamboo, Bioresource Technology 169 (2014) 313-319.

[8] R.E. Guedes, A.S. Luna, A.R. Torres, Operating parameters for bio-oil production in biomass pyrolysis: A review, Journal of Analytical and Applied Pyrolysis 129 (2018) 134-149.

[9] B.B. Uzun, A.E. Pütün, E. Pütün, Fast pyrolysis of soybean cake: Product yields and compositions, Bioresource Technology 97 (2006) 569-576.

[10] A. Pattiya, S. Suttibak, Production of bio-oil via fast pyrolysis of agricultural residues from cassava plantations in a fluidized-bed reactor with a hot vapour filtration unit, Journal of Analytical and Applied Pyrolysis 95 (2012) 227-235.

[11] R. Sharma, P.N. Sheth, Thermo-Chemical Conversion of Jatropha Deoiled Cake: Pyrolysis vs. Gasification, International Journal of Chemical Engineering and Applications 6 (2015) 376-380.

[12] K. Duanguppama, N. Suwapaet, A. Pattiya, Fast pyrolysis of contaminated sawdust in a circulating fluidised bed reactor, Journal of Analytical and Applied Pyrolysis 118 (2016) 63-74.

[13] C. Acikgoz, O. Onay, O.M. Kockar, Fast pyrolysis of linseed-product yields and compositions, Journal of Analytical and Applied Pyrolysis 71 (2004) 417-429.

[14] Z. Luo, S. Wang, Y. Liao, J. Zhou, Y. Gu, K. Cen, Research on biomass fast pyrolysis for liquid fuel, Biomass and Bioenergy 26 (2004) 455-462.

[15] R. Xu, L. Ferrante, C. Briens, F. Berruti, Flash pyrolysis of grape residues into biofuel in a bubbling fluid bed, Journal of Analytical and Applied Pyrolysis 86 (2009) 58-65.

[16] M.F. Demirbas, M. Balat, Biomass pyrolysis for liquid fuels and chemicals: A review, Journal of Scientific & Industrial Research 66 (2007) 797-804.

[17] A.V. Bridgwater, Review of fast pyrolysis of biomass and product upgrading, Biomass and Bioenergy 38 (2012) 68-94.

[18] Ö. Onay, S.H. Beis, Ö.M. Koçkar, Fast pyrolysis of rape seed in a well-swept fixed-bed reactor, Journal of Analytical and Applied Pyrolysis 58 (2001) 995-1007.

[19] D. Chen, Y. Li, K. Cen, M. Luo, H. Li, B. Lu, Pyrolysis polygeneration of poplar wood: Effect of heating rate and pyrolysis temperature, Bioresource Technology 218 (2016) 780-788.

[20] W.N.R.W. Isahak, M. W.M. Hisham, M.A. Yarmo, T.Y. Hin. A review on bio-oil production from biomass by using pyrolysis method, Renewable and Sustainable Energy Reviews 16 (2012) 5910-5923.

[21] B. Kang, K.H. Lee, H.J. Park, Y. Park, J. Kim, Fast pyrolysis of radiate pine in a bench scale plant with a fluidized bed: Influence of a char separation system and reaction conditions on the production of bio-oil, Journal of Analytical and Applied Pyrolysis 76 (2006) 32-37.

[22] J. Shen, X. Wang, M. Garcia-Perez, D. Mourant, M. J. Rhodes, C. Li, Effect of particle size on the fast pyrolysis of oil mallee woody biomass, Fuel 88 (2009) 1810-1817.

[23] R. Garg, N. Anand, D. Kumar, Pyrolysis of babool seeds (*Acacia nilotica*) in a fixed bed reactor and bio-oil characterization, Renewable Energy 96 (2016) 167-171.

[24] J. Davidson, D. Harrison, Fluidization, Academic Press, London and New York, 1971.

[25] P.N. Rowe, A.W. Nienow, Particle Mixing and Segregation in Gas Fluidised Beds: A Review, Powder Technology 15 (1976) 141-147.

[26] R. Bilbao, J. Lezaun, M. Menéndez, M.T. Izquierdo, Segregation of straw/sand mixtures in fluidized beds in non-steady state, Powder Technology 68 (1991) 31-35.

[27] A. Soria-Verdugo, L.M. García-Gutiérrez, S. Sánchez-Delgado, U. Ruiz-Rivas, Circulation of an object immersed in a bubbling fluidized bed, Chemical Engineering Science 66 (2011) 78-87.

[28] A. Soria-Verdugo, L.M. García-Gutiérrez, N. García-Hernando, U. Ruiz-Rivas, Buoyancy effects on objects moving in a bubbling fluidized bed, Chemical Engineering Science 66 (2011) 2833-2841.

[29] A. Soria-Verdugo, N. García-Hernando, J.A. Almendros-Ibáñez, U. Rivas-Ruiz, Motion of a large object in a bubbling fluidized bed with a rotating distributor, Chemical Engineering and Processing 50 (2011) 859-868.

[30] L. Lundberg, A. Soria-Verdugo, D. Pallarès, R. Johansson, H. Thunman, The role of fuel mixing on char conversion in a fluidized bed, Powder Technology 316 (2017) 677-686.

[31] R. Reschmeier, D. Roveda, D. Müller, J. Karl. Pyrolysis kinetics of wood pellets in fluidized beds, Journal of Analytical and Applied Pyrolysis 108 (2014) 117-129.

[32] A. Soria-Verdugo, A. Morato-Godino, L.M. García-Gutiérrez, N. García-Hernando, Pyrolysis of sewage sludge in a fixed and a bubbling fluidized bed - Estimation and experimental validation of the pyrolysis time, Energy Conversion and Management 144 (2017) 235-242.

[33] D. Kunii, O. Levenspiel, Fluidization Engineering, Wiley, New York, 1969.

[34] S. Koppatz, C. Pfeifer, H. Hofbauer, Comparison of the performance behavior of silica sand and olivine in a dual fluidised bed reactor system for steam gasification of biomass at pilot plant scale, Chemical Engineering Journal 175 (2011) 468-483.

[35] P.C. Carman, Fluid flow through granular beds, Transactions of the Institution of Chemical Engineers 15 (1937) 150-166.

[36] D. Geldart, Types of gas fluidization, Powder Technology (1973) 7, 285-292.

[37] J. Sánchez-Prieto, A. Soria-Verdugo, J. V. Briongos, D. Santana, The effect of temperature on the distributor design in bubbling fluidized beds, Powder Technology 261 (2014) 176-184.

[38] J.M. Encinar, J.F. González, J. González, Fixed bed pyrolysis of *Cynara cardunculus* L. Product yields and compositions, Fuel Processing Technology 68 (2000) 209-222.

[39] J.M. Encinar, J.F. González, J. González, Steam gasification of *Cynara cardunculus* L: influence of variables, Fuel Processing Technology 75 (2002) 27-43.

[40] T. Damartzis, D. Vamvuka, S. Sfakiotakis, A. Zabaniotou, Thermal degradation studies and kinetic modelin of cardoon (*Cynara cardunculus*) pyrolysis using thermogravimetric analysis (TGA), Bioresource Technology 102 (2011) 6230-6238.

[41] D. Serrano, M. Kwapinska, A. Horvat, S. Sánchez-Delgado, J.J. Leahy, *Cynara cardunculus* L. gasification in a bubbling fluidized bed: the effect of magnesite and olivine on product gas, tar and gasification performance, Fuel 173 (2016) 247-259.

[42] J. Gómez-Hernández, D. Serrano, A. Soria-Verdugo, S. Sánchez-Delgado, Agglomeration detection by pressure fluctuation analysis during Cynara cardunculus L. gasification in a fluidized bed, Chemical Engineering Journal 284 (2016) 640-649.

[43] J. Gominho, M.D. Curt, A. Lorenço, J. Fernández. H. Pereira. Cynara cardunculus L. as a biomass and multi-purpose crop: A review of 30 years of research, Biomass and Bioenergy 109 (2018) 257-275.

[44] A. Soria-Verdugo, E. Goos, A. Morato-Godino, N. García-Hernando, U. Riedel, Pyrolysis of biofuels of the future: Sewage sludge and microalgae - Thermogravimetric analysis and modelling of the pyrolysis under different temperature conditions, Energy Conversion and Management 138 (2017) 261-272.

[45] F. Johnsson, S. Andersson, B. Leckner, Expansion of a freely bubbling fluidized bed, Powder Technology 68 (1991) 117-123.

[46] A. Soria-Verdugo, A. Morato-Godino, L.M. Garcia-Gutierrez, N. Garcia-Hernando, Pyrolysis of sewage sludge in a bubbling fluidized bed: determination of the reaction rate, In: 12th International conference on fluidized bed technology (CFB 12), Krakow, Poland; 2017.

[47] Q. Yan, H. Toghiani, F. Yu, Z. Cai, J. Zhang, Effects of pyrolysis conditions on yield of bio-chars from pine chips, Forest Products Journal 61 (2011) 367-371.

[48] S. Samih, J. Chaouki. Development of a fluidized bed thermogravimetric analyzer, AIChE Journal 61 (2015) 84-89.

[49] P.A. Horne, P.T. Williams, Influence of temperature on the products from the flash pyrolysis of biomass, Fuel 78 (1996) 1051-1059.

[50] M. Asadullah, M.A. Rahman, M.M. Ali, M.A. Motin, M.B. Sultan, M.R. Alam, M.S. Rahman, Jute stick pyrolysis for bio-oil production in fluidized bed reactor, Bioresource Technology 99 (2008) 44-50.

[51] H.S. Heo, H.J. Park, Y.K. Park, C. Ryu, D.J. Suh, Y.W. Suh, J.H. Yim, S.S. Kim, Bio-oil production from fast pyrolysis of waste furniture sawdust in a fluidized bed, Bioresource Technology 101 (2010) 91-96.

[52] M. Coulson, A.V. Bridgwater. Fast pyrolysis of annually harvested crops for bioenergy applications, Proceeding of the 2nd World Conference on Biomass, vol. I, 2004, p. 1098.

[53] A. Demirbas, Effects of temperature and particle size on bio-char yield from pyrolysis of agricultural residues, Journal of Analytical and Applied Pyrolysis 72 (2004) 243-248.

[54] H.S. Choi, Y.S. Choi, H.C. Park, Fast pyrolysis characteristics of lignocellulosic biomass with varying reaction conditions, Renewable Energy 42 (2012) 131-135.

List of figures

Figure 1. Schematic of the experimental facility.

Figure 2. Minimum fluidization velocity of the silica sand particles as a function of reactor temperature.

Figure 3. (a) Time evolution of the percentage of mass remaining in the reactor and (b) time evolution of the conversion factor, during the pyrolysis of small particles of *Cynara cardunculus* L. with a bed temperature of 550 °C, for various excess gas velocities.

Figure 4. Time evolution of the percentage of mass remaining in the reactor during the pyrolysis of small particles of *Cynara cardunculus* L. for various excess gas velocities and bed temperatures.

Figure 5. Time evolution of the reaction rate during the pyrolysis of small particles of *Cynara cardunculus* L. for various excess gas velocities and bed temperatures.

Figure 6. (a) Total volatile matter released and (b) pyrolysis time for the pyrolysis of small particles of *Cynara cardunculus* L. as a function of the excess gas velocity for various reactor temperatures.

Figure 7. Time evolution of the reaction rate during the pyrolysis of *Cynara cardunculus* L. at 550 ºC for various excess gas velocities and particle sizes.

Figure 8. Total volatile matter released during the pyrolysis of *Cynara cardunculus* L. as a function of the excess gas velocity for various reactor temperatures and particles sizes.

Figure 9. Pyrolysis times of *Cynara cardunculus* L. as a function of the excess gas velocity for samples of different particle sizes and bed temperatures of 450, 550, and 650 °C.

List of tables

Table 1. Operating conditions used during the pyrolysis experiments.

Table 2. Characterization of *Cynara cardunculus* L. samples (ar: as received; db: dry basis; *: obtained by difference).

Table 3. Total volatile matter released and pyrolysis time for the pyrolysis of small particles of *Cynara cardunculus* L. at 550 °C, as a function of the excess gas velocity.

Table 4. Results of the fitting of the experimental results to the apparent kinetics model.